

Transient Infrared Characterization of Oxygen Storage Capability of Ce–Pd/Al₂O₃ Catalyst during NO–CO Reaction

Scott A. Hedrick, Steven S. C. Chuang,* Khalid Almusaiteer, and Robert W. Stevens, Jr.

The University of Akron, Department of Chemical Engineering, Akron, Ohio 44325-3906

Received: December 30, 2002

Oxygen storage and its effects on the adsorbates during NO–CO reaction have been studied by sequential pulsing of CO/O₂/CO into an NO–CO reactant stream over Pd/Al₂O₃ and Ce–Pd/Al₂O₃ catalysts. The adsorbates and reaction effluent were monitored concurrently by in situ infrared spectroscopy and mass spectrometry, respectively. It was found that the presence of ceria minimized the impact of O₂ and CO on the adsorbates over the Ce–Pd/Al₂O₃ catalyst at 673 K. This effect diminished at 573 and 473 K along with its storage capacity. Storage capacity is directly proportional to temperature in the range 473–673 K. Oxygen storage occurs differently in the presence of NO–CO than in an inert helium/argon environment, which has been used widely as the medium to study O₂ storage on ceria-based catalysts. The presence of the reactants and their adsorbates on the catalyst surface leads O₂ and CO to adsorb and react on the ceria surface prior to the Pd⁰ surface at 673 K. In addition, O₂ pulses at 573 and 473 K, unlike those at 673 K, decreased linear/bridged CO and linear NO on Pd⁰ without producing Pd⁺–NO, indicating that oxygen blocks adsorption sites on Pd without oxidizing Pd⁰ to Pd⁺. The active adsorbates for NO–CO decomposition are linear NO and linear/bridged CO on Pd⁰.

Introduction

The automobile three-way catalytic converter uses Pd, Pt, and Rh as key components in catalyzing NO reduction by CO, hydrocarbon oxidation, and CO oxidation.¹ These catalysts give an optimum conversion for NO, CO, and hydrocarbons (HC) for the flue gas produced from stoichiometric combustion at an air-to-fuel ratio (A/F) of 14.6.² However, this air-to-fuel ratio oscillates under practical conditions. Use of excess fuel in combustion produces flue gas containing more HC relative to O₂, providing a reducing (fuel-rich) environment for the catalyst, increasing NO conversion but decreasing HC and CO conversion. The presence of excess air from fuel-lean combustion in the flue gas produces an oxidizing environment, decreasing NO conversion but giving a high conversion for CO and HC oxidation.

One method that widens the A/F ratio window is the addition of ceria to the catalyst. Ceria has long been known to exhibit oxygen storage capability, allowing release of oxygen in a reducing environment and uptake of oxygen in an oxidizing environment.³ The key to this oxygen storage ability lies in the ease in which ceria is able to undergo changes in oxidation state, from CeO₂ (Ce⁴⁺) in an oxidizing environment to Ce₂O₃ (Ce³⁺) in a reducing environment and vice versa as shown by XPS studies.^{4,5} The benefits of oxygen storage include (i) enhancement of Pd catalyst effectiveness for the removal of NO, CO, and HC under oscillating A/F conditions, and (ii) promotion of the reaction of CO and/or HC with H₂O in the fuel-rich mode.⁶

Although oxygen storage capacity of ceria has been quantified in the literature,^{7–12} most measurements were done far from practical operating conditions. We have devised an approach to (i) determine the oxygen storage capability of Pd/Al₂O₃ and Ce–Pd/Al₂O₃ under conditions where the NO–CO reaction

takes place, and (ii) to determine the effect of oxygen storage on the adsorbates' reactivity during the NO–CO reaction. This approach involves pulsing CO and O₂ into the NO–CO reactant flow and then determining the responses of adsorbates by in situ infrared (IR) spectroscopy and the responses of gaseous reactants and products by mass spectrometry (MS). Pulsing CO into the NO–CO flow over the catalyst creates a reducing environment for the catalyst, causing the withdrawal of stored oxygen from the catalyst to form CO₂; pulsing O₂ into the NO–CO flow produced an oxidizing environment, causing oxidation of the reductants (i.e., CO and HC) and the uptake of oxygen by the catalyst. The amount of stored oxygen available for the reaction with CO in the reducing environment can be quantified by measuring CO₂ formation as well as CO/O₂ conversion during CO and O₂ pulsing. The effect of oxygen storage on the adsorbates and their reaction pathways can be elucidated from MS responses of gaseous reactants/products and IR responses of adsorbates. This paper addresses the role of ceria in altering the effect of oxygen on the adsorbates and the catalyst activity; this paper also underscores the importance of oxygen storage measurement under practical reaction conditions.

Experimental Section

Catalyst Preparation and Characterization. A 2 wt % Pd/Al₂O₃ catalyst was prepared by incipient wetness impregnation of γ -Al₂O₃ support (Alfa Chemicals, 100 m²/g) with a PdCl₂ (Alfa Chemicals) solution at a pH of 2.8 and a temperature of 333 K. The catalyst was calcined in flowing air at 673 K for 8 h and then reduced in flowing hydrogen at 673 K for 8 h. The Pd loading on the Pd/Al₂O₃ catalyst was determined to be 1.75 wt % by inductively coupled plasma (ICP) analysis (Galbraith Laboratories, Inc.). X-ray diffraction (XRD) yielded an average Pd crystallite size of 6.4 nm, corresponding to a dispersion of 10%. Ce–Pd/Al₂O₃ (2 wt % Pd, 20 wt % Ce) was prepared by coimpregnation with a Ce(NO₃)₃ and PdCl₂ solution. XRD data

* Author to whom correspondence should be addressed.

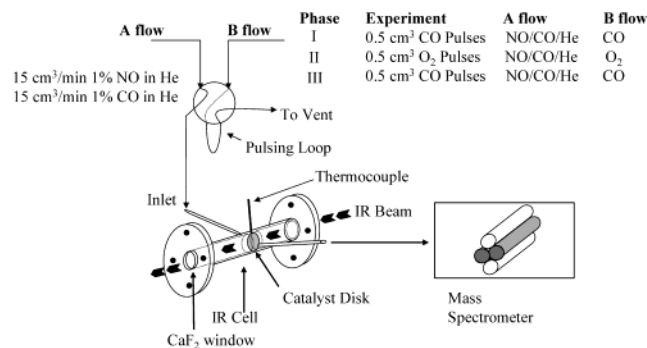


Figure 1. Experimental approach.

yielded an average Pd crystallite size of 5.2 nm, corresponding to a dispersion of 12%.

Reaction Studies. The experimental apparatus, including an in situ IR reactor cell with CaF₂ windows, has been reported in detail elsewhere.¹³ A schematic of the experimental setup used in this study is outlined in Figure 1. For each experiment, a total of 143 mg of fresh catalyst was used with approximately 15 mg of this total pressed into a self-supporting disk and placed in the path of the IR beam. The remainder of the catalyst was placed in the vicinity of the disk for the purpose of increasing conversion. Prior to each experiment, the catalyst was heated in flowing He at 673 K. The reaction was carried out at 473, 573, and 673 K and 0.1 MPa at a total flow rate of 30 cm³/min with each run carried out on fresh catalyst. The reactant mixture consisted of equimolar flows of 1 vol % NO in He and 1 vol % CO in He. Upon reaching steady-state reaction, a series of 0.5 cm³ CO and O₂ pulses were introduced into the NO–CO reactant flow by a 6-port valve as depicted in Figure 1. Flow “A” represents the NO/CO reaction mixture, and flow “B” represents the species being pulsed into A.

The first series of pulses into the NO–CO flow is CO, which follows the sequence of Phase I as shown in Figure 1. The objective of this series of CO pulses is to deplete kinetically accessible oxygen on the catalyst by reacting to produce CO₂. CO pulses were made until all reactants, products, and adsorbates gave the same subsequent responses, indicating that all the kinetically accessible oxygen available for reaction had reacted. After these pulses, 0.5 cm³ pulses of 100% O₂ (Phase II in Figure 1) were introduced into the reaction mixture to saturate the surface with adsorbed oxygen and to determine its effect on adsorbates and catalyst activity. Pulsing continued until the catalyst was no longer able to uptake oxygen as evidenced by oxygen breakthrough, which gave the same size O₂ peak for subsequent O₂ pulses in the MS profile. CO pulses were again introduced (Phase III), as shown in Figure 1, to react with the stored oxygen deposited from the O₂ pulses.

IR spectra were collected during each pulse by a Nicolet Magna 550 spectrometer equipped with an MCT-B detector at a resolution of 4 cm⁻¹. Gaseous effluent was monitored by a Balzers QMG 112 mass spectrometer for experiments with Pd/Al₂O₃ and by a Prisma QMS 200 mass spectrometer for experiments with Ce–Pd/Al₂O₃. We monitored the following *m/e* ratios: 4 (He), 12 (CO), 22 (CO₂), 28 (CO and N₂), 30 (NO), 32 (O₂), 44 (CO₂ and N₂O), and 46 (NO₂). The contribution of CO₂ and N₂O to *m/e* = 44 can be resolved by CO₂ calibration which shows that the area of the 44 peak is 41.6 times the area of the *m/e* = 22 peak for any given CO₂ pulse. The contribution of CO and N₂ to the *m/e* = 28 was resolved by calibrating the intensity ratio of *m/e* = 28 to *m/e* = 14 for N₂. The amount of CO₂ and N₂O produced as well as

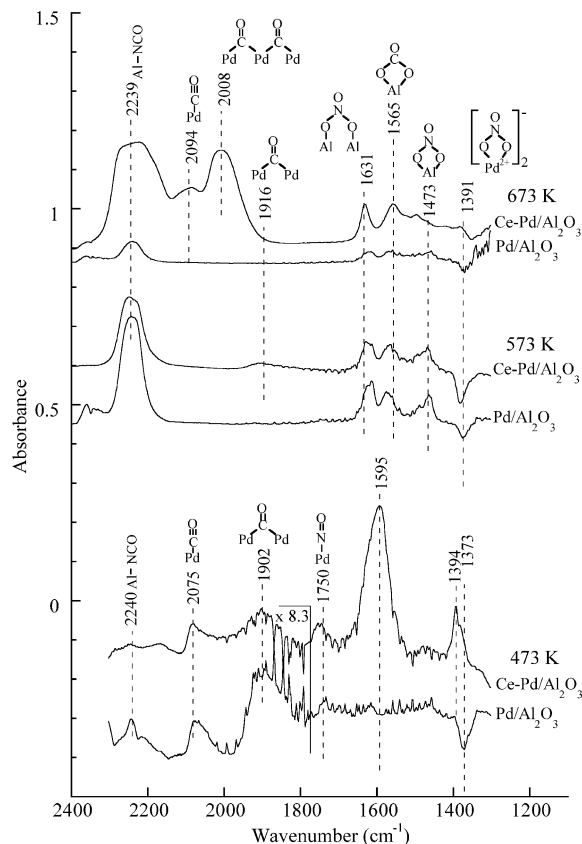


Figure 2. IR spectra and band assignments for 1% NO/1% CO flow over Ce–Pd/Al₂O₃ and Pd/Al₂O₃ under steady conditions prior to pulsing at 673, 573, and 473 K.

TABLE 1: Steady-State NO Conversion

temperature (K)	NO conversion (%)	
	Ce–Pd/Al ₂ O ₃	Pd/Al ₂ O ₃
673	100	100
573	75	95
473	55	37

the amount of CO consumed during CO and O₂ pulses was quantified by multiplying the area under the *m/e* response curve by its responding factor. As a result of the relatively low response factor of N₂ at *m/e* = 14, the amount of N₂ produced during the pulses can be not accurately determined.

Results

Table 1 lists the NO conversion on Pd/Al₂O₃ and Ce–Pd/Al₂O₃ at 473, 573, and 673 K. The steady-state NO conversion increased with temperature on both catalysts. The activities of both catalysts did not change over the course of each experiment at each respective temperature. NO conversion on Ce–Pd/Al₂O₃ is less sensitive to temperature in the range 473–673 K than on Pd/Al₂O₃. The results suggest that the reaction over Ce–Pd/Al₂O₃ has a lower activation energy than over Pd/Al₂O₃. Similarly, addition of ceria to a Rh/Al₂O₃ catalyst was found to cause a reduction in activation energy.¹⁴

Figure 2 compares the IR spectra of the steady-state NO–CO reaction, corresponding to the NO conversion listed in Table 1. The steady-state reaction at 473 K produced linear CO at 2075 cm⁻¹, bridged CO at 1902 cm⁻¹, and linear NO on Pd⁰ at 1750 cm⁻¹ on both catalysts as well as a very strong bidentate carbonate band on Ce–Pd/Al₂O₃ at 1595 cm⁻¹. The prominent bands, i.e., linear CO, bridged CO, linear NO, and carbonate,

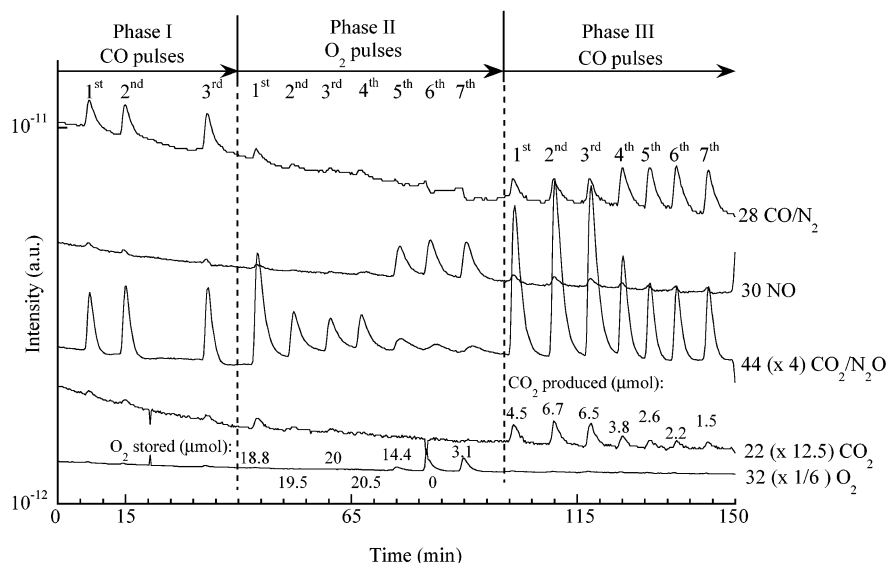


Figure 3. CO/O₂ pulsing into 1% NO/1% CO flow over Ce–Pd/Al₂O₃ at 673 K. The amount of oxygen stored and CO₂ produced are listed along with the Phase II O₂ and Phase III CO₂ pulses, respectively.

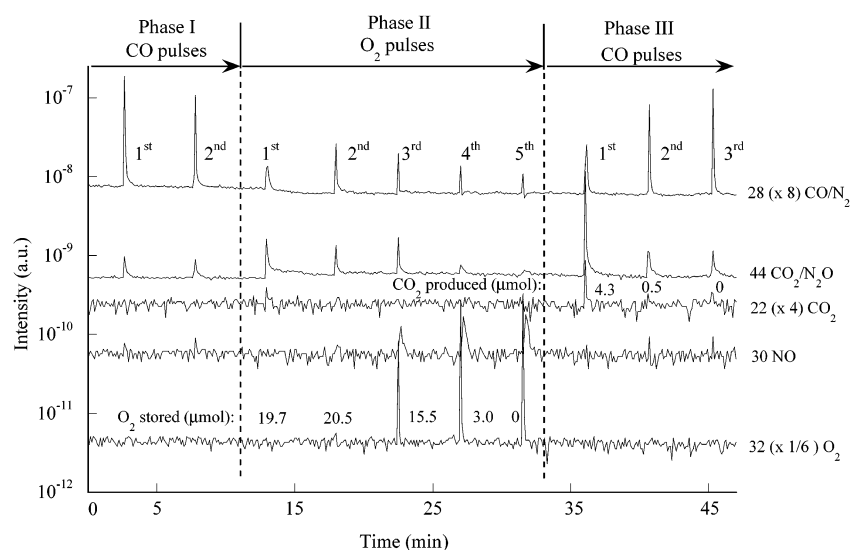


Figure 4. CO/O₂ pulsing into 1% NO/1% CO flow over Pd/Al₂O₃ at 673 K. The amount of oxygen stored and CO₂ produced are listed along with the Phase II O₂ and Phase III CO₂ pulses, respectively.

produced at 473 K were not observed on either catalyst at 573 K, indicating that the rates of conversion of these species are greater than their formation rates. The Al–NCO at 2239 cm⁻¹, bidentate nitrate at 1631 cm⁻¹, carbonate at 1565 cm⁻¹, and chelating nitrate at 1473 cm⁻¹ emerged on both catalysts at 573 K. The commonality of the carbonate and nitrate bands on both catalysts indicates that these species are most likely adsorbed on the support. These band assignments are well established in the literature.^{15–24}

At 673 K, the Ce–Pd/Al₂O₃ catalyst produced linear CO at 2094 cm⁻¹ and a new band at 2008 cm⁻¹ which has been assigned as a compressed bridged CO species.²⁵ Because the reaction achieved nearly complete conversion at this temperature, the presence of these species suggests that these species are in excess with respect to adsorbed NO on the catalyst surface.

Figures 3 and 4 show the MS transient responses for the entire experimental run at 673 K on Ce–Pd/Al₂O₃ and Pd/Al₂O₃, respectively, providing an overall picture of CO and O₂ pulses and their product responses. Figure 3 shows that the first CO pulse in Phase I produced CO₂ and N₂O, as evidenced by peaks

at *m/e* = 22 and 44. A positive peak indicates an increase in the concentration of each species with respect to the steady-state concentration. The positive peak at *m/e* = 30, corresponding to an increase in NO concentration, indicates a decrease in the NO conversion as a result of the CO pulse. The amounts of CO₂ and N₂O produced as well as the amount of CO consumed for each CO and O₂ pulse are listed in Table 2. The amount of CO₂ estimated from the peak area of the *m/e* = 22 curve should be considered as a lower limit as a result of the high baseline of CO₂ produced from the NO–CO reaction. The shift in the CO baseline in Phase I in Figure 3 may lead to an overestimation of CO consumption. The second and third CO pulses produced nearly identical MS responses to the first pulse, suggesting that the amount of oxygen available for the reaction with each of these CO pulses was the same.

The first O₂ pulse in the Phase II sequence resulted in peaks at *m/e* = 22, 28, 30, and 44, indicating increases in the formation of CO₂/N₂O as well as a decrease in NO conversion. Subsequent pulses (i) produced smaller amounts of CO₂ as indicated by decreases in the *m/e* = 22 and 44 peaks, (ii) decreased the rate of NO conversion as shown by increases in the NO peaks, and

TABLE 2: Quantification of CO₂, N₂O, CO, and O₂ for CO and O₂ Pulses on Ce–Pd/Al₂O₃ and Pd/Al₂O₃ at 673 K

pulse	CO ₂ produced (μmol)	N ₂ O produced (μmol)	CO consumed (μmol)	O ₂ consumed (μmol)	O ₂ stored (μmol)
Ce–Pd/Al ₂ O ₃					
Phase I					
1st CO	1.1	0.5	2.1		
2nd CO	0.8	0.7	1.5		
3rd CO	0.5	0.4	0.3		
Phase II					
1st O ₂	3.3	1.4	--	20.5	18.8
2nd O ₂	1.8	0.5	--	20.5	19.5
3rd O ₂	0.8	0.8	--	20.5	20.0
4th O ₂	0	1.1	--	20.5	20.5
5th O ₂	0	0.7	--	14.4	14.4
6th O ₂	0	0.7	--	0	0
7th O ₂	0	0.7	--	3.1	3.1
Phase III					
1st CO	4.5	1.7	7.2		
2nd CO	6.7	1.8	8.0		
3rd CO	6.5	1.8	7.2		
4th CO	3.8	0.2	4.0		
5th CO	2.6	0	2.8		
6th CO	2.2	0.2	2.5		
7th CO	1.5	0.5	1.5		
Total					96.3
Pd/Al ₂ O ₃					
Phase I					
1st CO	0	0.4	0		
2nd CO	0	0.4	7.3		
Phase II					
1st O ₂	1.6	0.7		20.5	19.7
2nd O ₂	0	0.5		20.5	20.5
3rd O ₂	0	0.6		15.5	15.5
4th O ₂	0	0.2		3.0	3.0
5th O ₂	0	0.2		0	0
Phase III					
1st CO	4.3	1.6	8.0		
2nd CO	0.5	0.3	4.8		
3rd CO	0	0.6	1.1		
Total					58.7

(iii) eventually led to oxygen breakthrough at the fifth O₂ pulse. The oxygen introduced to the catalyst in a pulse should follow one of three paths: (i) oxygen storage, (ii) reaction with CO to form CO₂, or (iii) departure from the reactor as part of the effluent. Thus, the amount of oxygen stored from each O₂ pulse can be obtained from the following mole balance:

$$\text{Mol O}_2 \text{ stored} = \text{Mol O}_2 \text{ in} - \text{Mol O}_2 \text{ out} - \frac{1}{2} \text{Mol CO}_2 \text{ produced}$$

These quantities are listed in Table 2 and Figures 3 and 4 along with the O₂ MS profiles. The sixth and seventh O₂ pulses produced the same MS responses, suggesting that the catalyst surface had become saturated with oxygen. Upon saturation, the O₂ pulses resulted in an inhibition of the NO–CO reaction as indicated by the emergence of the prominent NO peak on the fifth and subsequent pulses.

Following saturation of the catalyst with stored oxygen, CO pulses were again introduced to react with the stored oxygen (Phase III). The stored oxygen reacted with the CO pulse, producing CO₂. The initial CO pulse produced a significant amount of additional CO₂ relative to the Phase I CO pulses. By the fifth CO pulse of Phase III, the amount of CO₂ decreased to the same level as the CO pulses introduced during Phase I, indicating that all stored oxygen introduced from the O₂ pulses in Phase II has been depleted.

Figure 4 shows that Pd/Al₂O₃ took a significantly lower number of O₂ pulses in Phase II to saturate the catalyst surface with oxygen than Ce–Pd/Al₂O₃; Pd/Al₂O₃ also took less CO to restore the initial CO response than Ce–Pd/Al₂O₃. This observation revealed that the ceria component on Ce–Pd/Al₂O₃ is capable of enhancing oxygen uptake during O₂ pulses.

To gain insight into the reaction involving CO and O₂ pulses, the IR spectra collected during the first CO pulse in Phase I were plotted in Figure 5. Prior to the CO pulse, the NO–CO reaction produced Al–NCO at 2250 cm⁻¹, linear CO at 2093 cm⁻¹, compressed bridged CO at 2012 cm⁻¹, bidentate nitrate at 1630 cm⁻¹, and bridged carbonate at 1560 cm⁻¹. As described earlier, the presence of adsorbed CO on Pd⁰ surface indicates these species are in excess with respect to adsorbed NO on the catalyst surface. This excess adsorbed CO appears to keep the catalyst surface in the reduced state. Further addition of CO by pulsing did not produce any appreciable change in the intensity of the adsorbates. The intensity of a number of prominent bands was plotted as a function of time along with the MS profiles in Figure 5b,c. The major effect of the CO pulse was to increase the formation of CO₂ and N₂O. The subsequent CO pulses gave the same responses as the first CO pulse.

The MS profiles of reactants/products as well as IR profiles of the specific adsorbates for the first CO pulse in Phase I (Figure 5b,c) on Ce–Pd/Al₂O₃ were plotted along with selected O₂ pulses in Phase II and CO pulse in Phase III in Figures 6 and 7 to highlight the effect of oxygen storage on the adsorbates' reactivity. The first O₂ pulse led to the formation of a significant amount of CO₂ and N₂O, but little changes in adsorbate intensity. Figures 6 and 7 show that the IR intensities of adsorbates after the first O₂ pulse are virtually the same as those following CO pulses in Phase I. The significant changes in the adsorbate intensities were observed during the second O₂ pulse, which caused emergence of linear NO on Pd⁺ at 1795 cm⁻¹ (Figure 6) and a decrease in the nitrate and carbonate intensities (Figure 7). The second O₂ pulse also dramatically reduced the intensities of linear CO, compressed bridged CO, and Al–NCO.

Subsequent O₂ pulses, as represented by the seventh O₂ pulse in Figures 6 and 7, caused (i) an increase in linear NO on Pd⁺, (ii) further diminution of linear CO (i.e., Pd⁰–CO), compressed bridged CO, and Al–NCO, and (iii) decreases in NO conversion as evidenced by increases in the NO profile. The observation of the depletion of Pd⁰–O and the formation of Pd⁺–NO is a strong indication that all the Pd surface atoms are oxidized as the catalyst surface becomes saturated with oxygen.

The first CO pulse in Phase III following the saturation of the catalyst surface with oxygen produced significantly more CO₂ than the first CO pulse in Phase I. This enhanced CO₂ production is a clear indication that the stored oxygen on the catalyst surface is active for reaction with the CO coming from the CO pulse. However, like the first O₂ pulse in Phase II, the first CO pulse had no impact on the adsorbates. The significant variation of adsorbate intensity was observed during the second CO pulse which gave rise to linear CO at 2055 cm⁻¹, bridged CO at 1904 cm⁻¹, Al–NCO, carbonate, and nitrate species. The IR spectra for adsorbed CO here are vastly different from those given for the initial CO pulse in Phase I, suggesting oxygen treatment severely modified the catalyst surface. The major effects of the CO pulses are to eliminate the Pd⁺–NO species and to promote the formation of Pd⁰–CO and bridged CO species, indicating that Pd⁺ is converted to Pd⁰.

Figures 8 and 9 show the MS and IR profiles for CO and O₂ pulses on Pd/Al₂O₃ and are analogous to Figures 6 and 7. The CO pulses in Phase I caused an increase in N₂O and Al–NCO

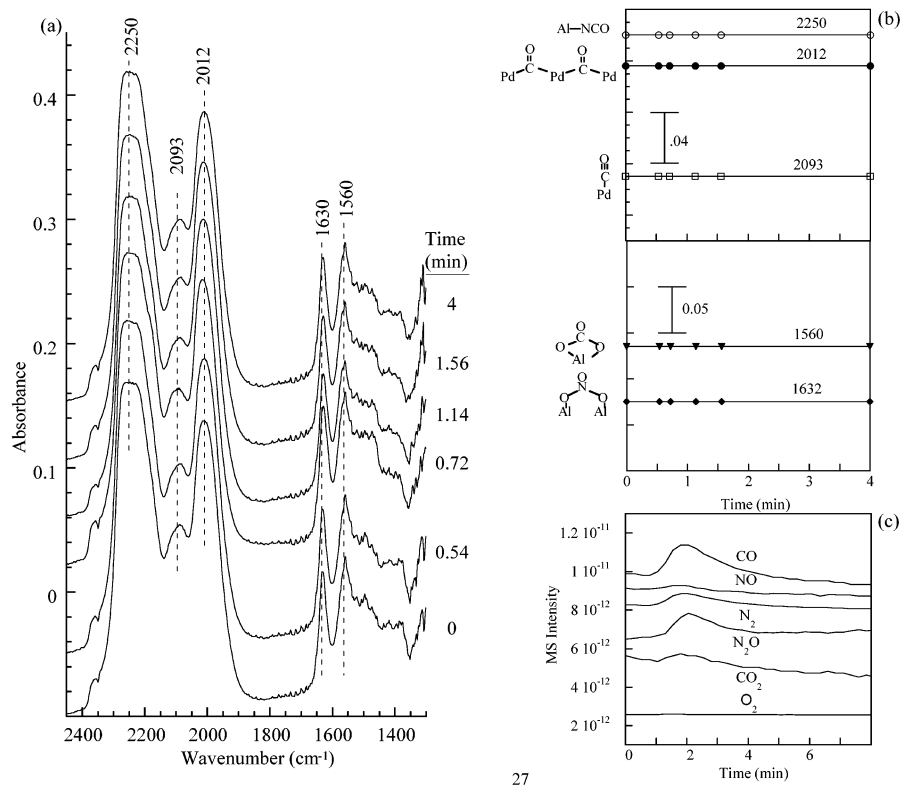


Figure 5. IR spectra and MS profiles for the first CO pulse in Phase I over Ce-Pd/Al₂O₃ at 673 K.

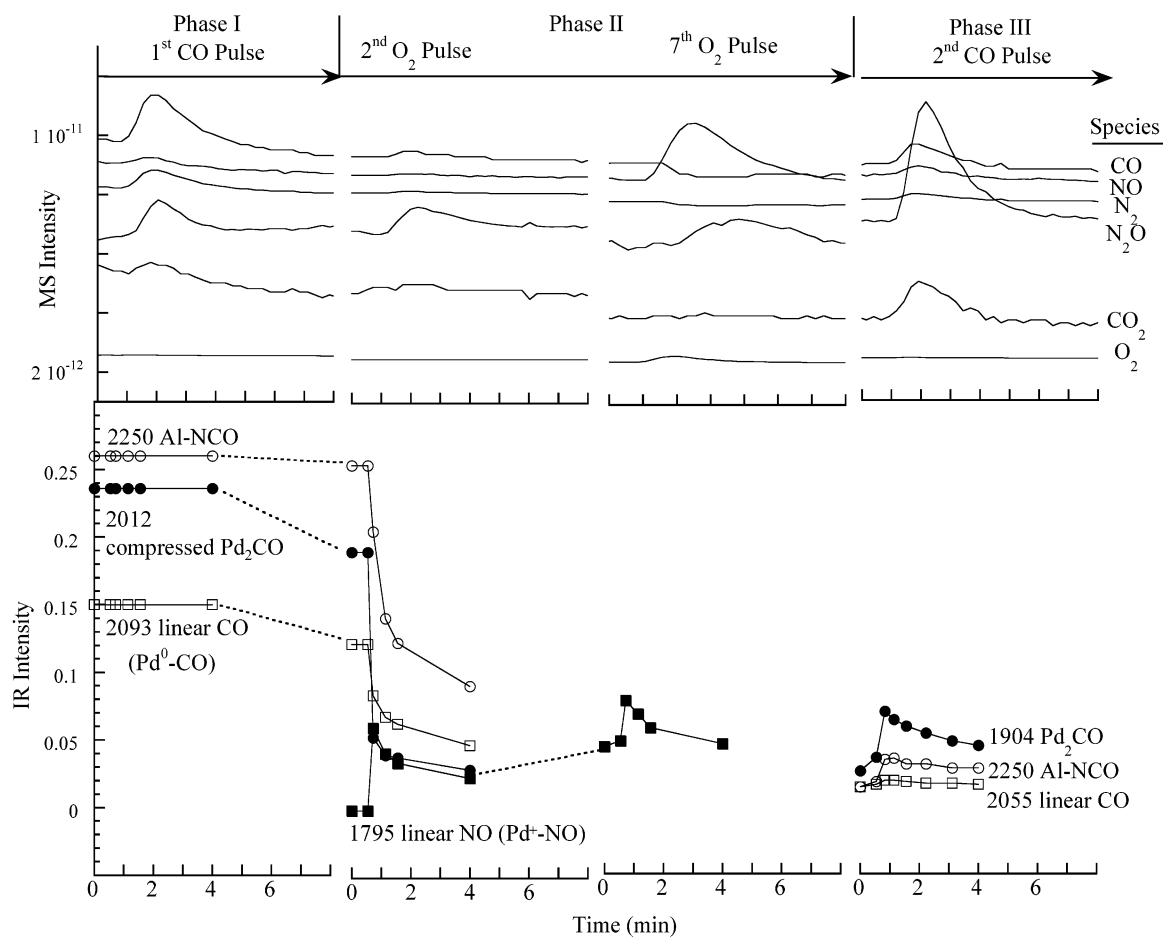


Figure 6. MS profiles and IR adsorbate intensities as a function of time for selected CO/O₂ pulses in each phase over Ce-Pd/Al₂O₃ at 673 K. Adsorbates shown are those above 1700 cm⁻¹.

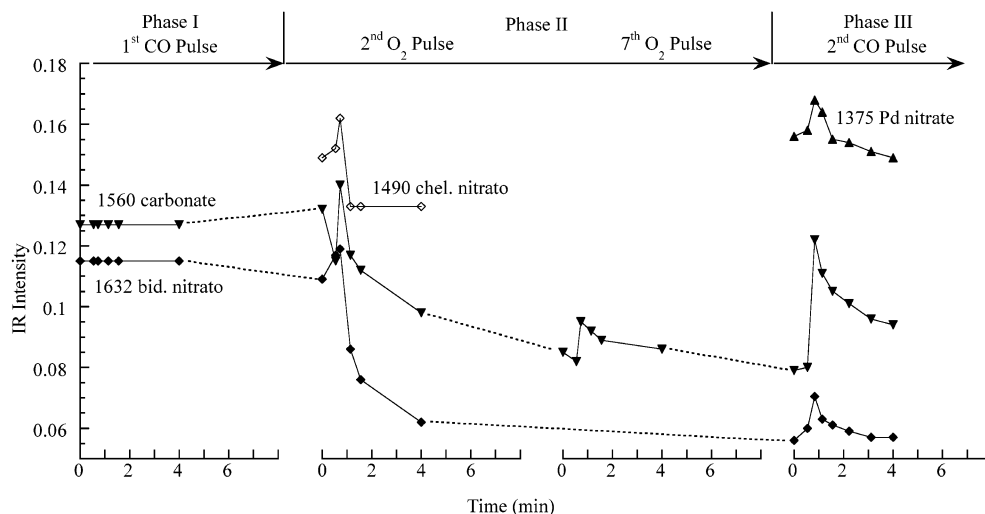


Figure 7. IR adsorbate intensities as a function of time for selected CO/O₂ pulses in each phase over Ce–Pd/Al₂O₃ at 673 K. Adsorbates shown are those below 1700 cm⁻¹.

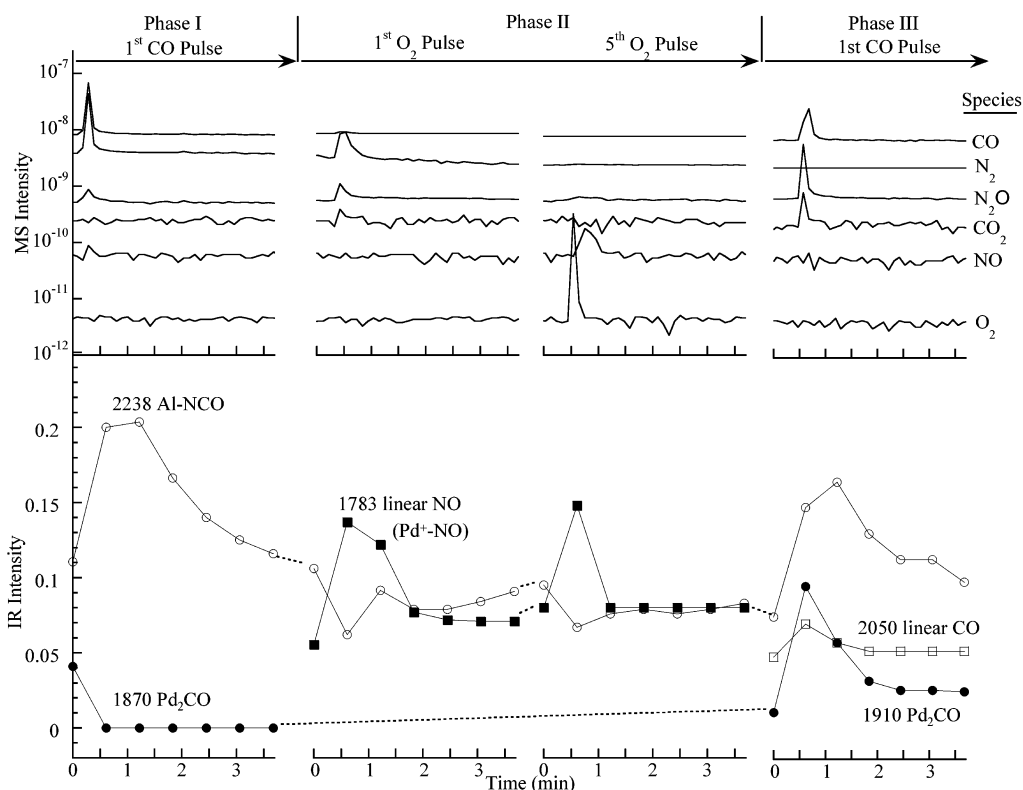


Figure 8. MS profiles and IR adsorbate intensities as a function of time for selected CO/O₂ pulses in each phase over Pd/Al₂O₃ at 673 K. Adsorbates shown are those above 1700 cm⁻¹.

formation. The absence of an increase in CO₂ formation suggests the lack of excess oxygen on catalyst surface. The first O₂ pulse in Phase II caused increases in CO₂, N₂O, and Pd⁺–NO concentration, but decreased IR intensity of Al–NCO and nitrate species. This is in contrast to the first O₂ pulse over Ce–Pd/Al₂O₃ which did not lead to any appreciable change in intensity of adsorbates. Subsequent O₂ pulses gave a similar IR response, caused a decrease in NO conversion, but little variation in CO₂ concentration.

The first CO pulse in Phase III produced substantially more CO₂ formation than the CO pulses during Phase I. This CO pulse also produced linear CO at 2050 cm⁻¹ and bridged CO at 1910 cm⁻¹ as well as eliminated Pd⁺–NO, reflecting the reduction of Pd⁺ to Pd⁰.

The same experimental sequences were carried out over both catalysts at 573 and 473 K. Figure 10 shows the IR spectra, MS profiles, and relative adsorbate peak heights as a function of time for the first CO pulse in Phase I on Ce–Pd/Al₂O₃ at 473 K. This CO pulse elicits substantial increases in both linear and bridged CO with a concomitant reduction in linear NO. All other adsorbates including nitrate and carbonate species remained constant during the pulse. The MS profiles show that CO pulsing produced CO₂/N₂O and caused a small decrease in NO conversion.

The MS profiles of reactants/products as well as IR profiles of the specific adsorbates for the first CO pulse in Phase I (Figure 10b,c) were plotted along with selected O₂ pulses in Phase II and CO pulse in Phase III in Figure 11. The major

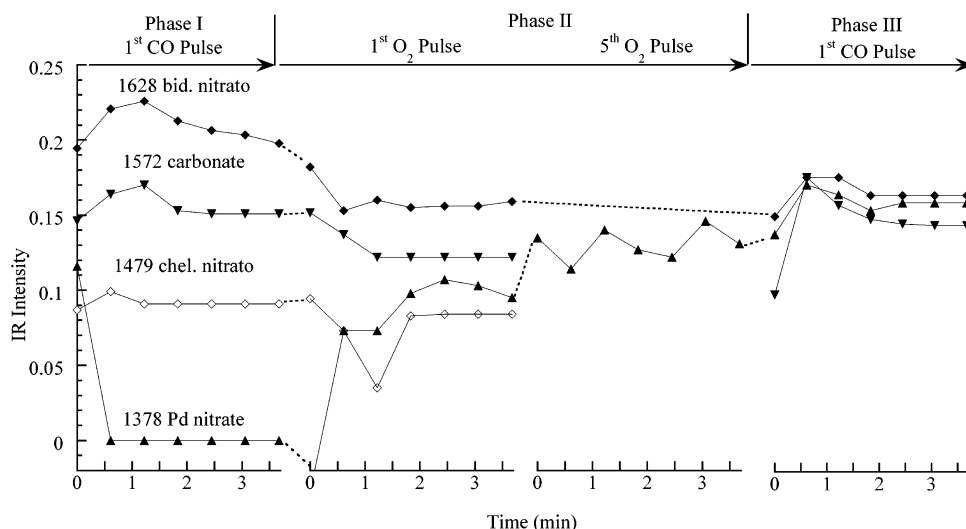


Figure 9. IR adsorbate intensities as a function of time for selected CO/O₂ pulses in each phase over Pd/Al₂O₃ at 673 K. Adsorbates shown are those below 1700 cm⁻¹.

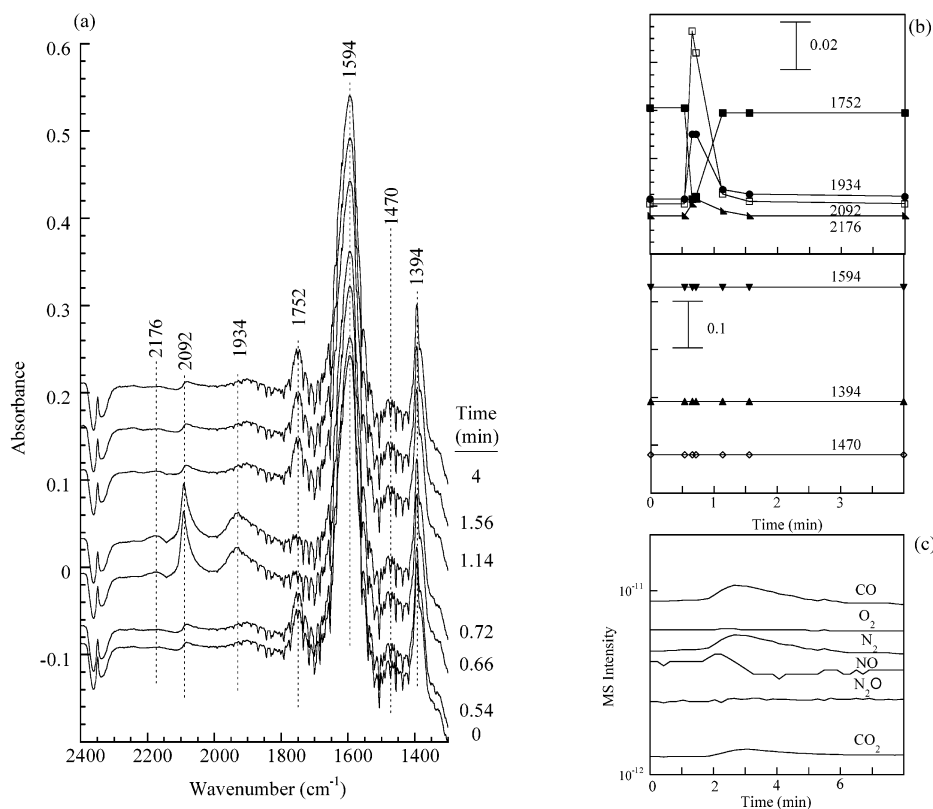


Figure 10. IR spectra and MS profiles for the first CO pulse in Phase I over Ce-Pd/Al₂O₃ at 473 K.

differences between CO and O₂ pulses at 473 and 673 K are the absence of oxygen storage and the lack of variation in nitrate and carbonate intensities at 473 K as shown in Figure 12. Because the conversion of NO is at a level of 55%, the Pd surface is populated with adsorbed CO and NO, reflecting that the rate of adsorption of NO and CO is higher than the rate of conversion of these species. The major effect of the CO pulse is to displace linear NO with linear and bridged CO, causing a decrease in NO conversion as evidenced by an increase in NO concentration during CO pulses.

The first O₂ pulse at 473 K in Figure 11, unlike its counterpart at 673 K, caused an immediate decrease in NO conversion, as evidenced by the peak at $m/e = 30$. This O₂ pulse also caused a decrease in linear CO at 2092 cm⁻¹, bridged CO at 1934 cm⁻¹,

and linear NO at 1752 cm⁻¹. Unlike the results on Ce-Pd/Al₂O₃ at 673 K, no formation of the Pd⁺-NO at 1790 cm⁻¹ was observed, although a slight, temporary blue shift in the Pd⁰-NO peak was observed, indicating that the Pd sites briefly carried a slightly positive charge. This indicates that the O₂ pulses on Ce-Pd/Al₂O₃ at 473 K act to block adsorption sites for NO and CO rather than oxidize the surface. The NO site-blocking effect brought about by O₂ decreased with consecutive O₂ pulses. By the thirteenth O₂ pulse, the O₂ pulse inhibited the conversion of Pd⁰-NO more than blocked the NO adsorption sites, resulting in a slight increase in Pd⁰-NO intensity during the O₂ pulse. CO pulses in Phase III produced adsorbates similar to those in Phase I, suggesting the O₂ pulse did not lead to significant modification of the catalyst surface at this

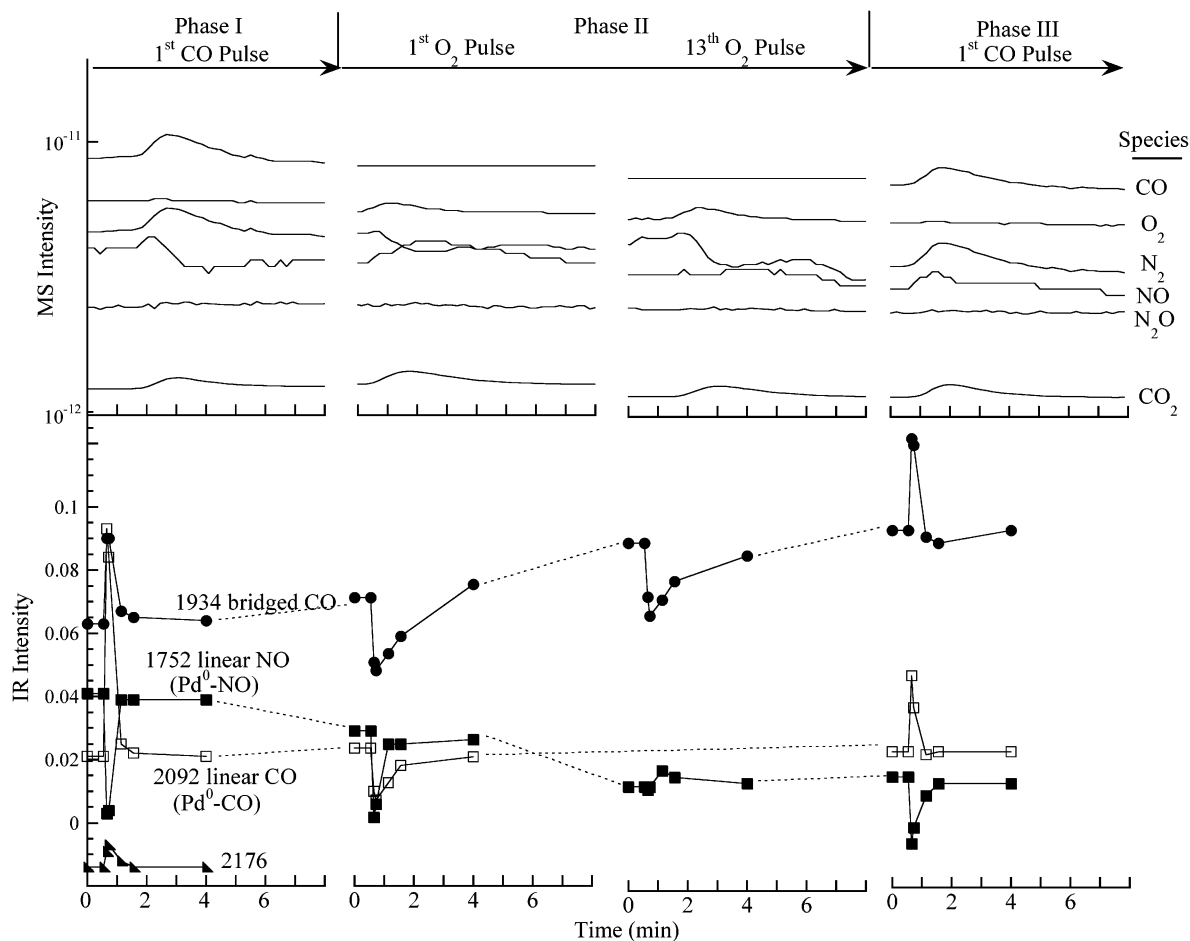


Figure 11. MS profiles and IR adsorbate intensities as a function of time for selected CO/O₂ pulses in each phase over Ce–Pd/Al₂O₃ at 473 K. Adsorbates shown are those above 1700 cm⁻¹.

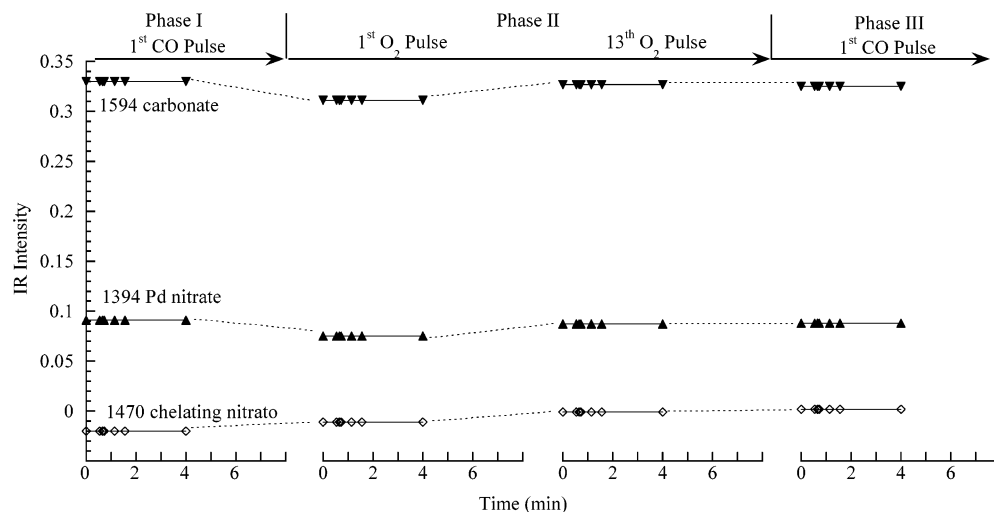


Figure 12. IR adsorbate intensities as a function of time for selected CO/O₂ pulses in each phase over Ce–Pd/Al₂O₃ at 473 K. Adsorbates shown are those below 1700 cm⁻¹.

temperature. Although adsorbed CO and NO on Pd/Al₂O₃ exhibited different intensities from those on Ce–Pd/Al₂O₃, their dynamic behaviors during CO and O₂ pulses are very similar on both catalysts.

Discussion

The significant difference in adsorbate and oxygen storage behaviors during O₂/CO pulses at 473 and 673 K demonstrates

that oxygen storage and its impact on the catalysis of the NO–CO reaction is a kinetic phenomenon which should be measured under practical reaction conditions. It is expected that oxygen may interact and react with the adsorbed species and catalyst surface at different rates under different reaction conditions. A critical question to be addressed is what is the reaction pathway for oxygen uptake and withdrawal. As a result of the inability of in situ infrared spectroscopy to directly observe the behavior

of adsorbed oxygen and its pathway, the reaction pathway of oxygen has to be elucidated from the variation in IR-observable adsorbates and reactant/product profiles during O₂ and CO pulses.

The Role of Ceria in the NO–CO Reaction. Results in Figures 3 and 4 show that CO pulses in Phase I withdrew any kinetically accessible oxygen by reaction to produce CO₂. These CO pulses rendered the Pd surface to the reduced state, which chemisorbs CO as linear and bridged CO and gives a strong Al–NCO intensity. A high concentration of CO, which keeps the catalyst surface in the reduced state, is evidenced by a high Al–NCO intensity. Isocyanate has been observed in a number of NO–CO reaction studies on Pd and Rh catalysts.^{21–23,26–28} The species that are associated with a reducing environment and reduced catalyst surface are depleted by O₂ pulses that produced Pd⁺–NO at 673 K. Thus, the intensity of adsorbed species such as Pd⁰–CO (i.e., linear CO), bridged CO, and Al–NCO can serve as an index of the Pd surface state.

The absence of variation of linear/bridged CO and Al–NCO during the first O₂ pulse over Ce–Pd/Al₂O₃ at 673 K shows that the O₂ from this pulse adsorbs on surface sites that are not associated with these adsorbed species. The substantial decrease in intensity of these species and increase in intensity of Pd⁺–NO began with the second O₂ pulses, revealing oxidation of Pd⁰ to Pd⁺. These observations showed that O₂ adsorbs and reacts with ceria before oxidizing Pd⁰ to Pd⁺. This observation is in contrast to the proposed role of noble metals in assisting oxygen spillover from the metal to Ce₂O₃ for the reaction: Ce₂O₃ + 1/2O₂ → 2CeO₂.^{7,10} However, an oxygen exchange study using ¹⁶O₂, ¹⁸O₂, and ¹⁶O¹⁸O over Pt/Al₂O₃ and Pt/CeO₂ at 673 K revealed that oxygen exchange did not proceed via Pt, but occurred directly on ceria.³ A bifunctional oxygen reaction pathway, which included both direct adsorption of O₂[–](g) on both ceria sites and metal sites, has also been proposed.²⁹ Furthermore, O₂ adsorption on metal sites can be strongly suppressed by adsorbed CO.³⁰

During the NO–CO reaction at 673 K, the presence of adsorbed NO/CO and their decomposition products on the Pd surface may lead oxygen to adsorb on the Ce₂O₃ surface prior to the Pd⁰ surface. In the absence of ceria, the O₂ pulse into NO/CO over Pd/Al₂O₃ led to an immediate alteration of adsorbates on the Pd surface. Thus, it can be concluded that the major role of ceria on Ce–Pd/Al₂O₃ catalyst is to uptake oxygen and minimize its impact on the adsorbates on the Pd surface during the initial O₂ pulses. This ceria effect is diminished at 573 and 473 K in which the first O₂ pulse alters the intensity of adsorbates on the Pd surface for both Pd/Al₂O₃ and Ce–Pd/Al₂O₃ (see Figure 11). The O₂ pulses at 473 K (shown in Figure 11) decreased linear/bridged CO and linear NO on Pd⁰ without producing Pd⁺–NO, indicating that oxygen blocks the Pd sites for CO and NO adsorption without oxidizing Pd⁰ to Pd⁺.

The oxygen uptake on ceria has been found to increase with temperature,^{3,10,31} which is consistent with our results. In their CO/O₂ pulsing into He study, Yao and Yu Yao found that oxygen storage capacity of CeO₂/Al₂O₃ at 573 K was nil and at 673 K was very limited (0.0003 μmol O₂/μmol CeO₂).¹⁰ However, addition of a metal (Pd, Pt, or Rh) to the ceria facilitated the oxygen storage capacity at temperatures from 573 to 773 K. Most studies typically characterized the oxygen storage capability of ceria in an ideal, i.e., inert, environment, typically He, but the presence of NO/CO and their adsorbates under reaction conditions complicates the reaction pathway of

TABLE 3: Percent Decreases in NO Conversion during Phase I CO Pulses

temperature (K)	NO conversion decrease (%)	
	Ce–Pd/Al ₂ O ₃	Pd/Al ₂ O ₃
673	1.5	8.3
573	2.1	0
473	4.7	0

oxygen and makes extrapolation of the results obtained from ideal conditions to practical conditions unreliable.

Ceria minimizes the impact of not only initial O₂ pulses but also CO pulses on the adsorbates. Significant increases in linear/bridged CO and Al–NCO were observed immediately following the CO pulse in Phase III over Pd/Al₂O₃. In contrast, these species began reemerging following the second and third CO pulse over Ce–Pd/Al₂O₃. The initial CO pulse, much like the initial O₂ pulse, produced CO₂ without altering the intensity of adsorbates on the Pd surface of the Ce–Pd/Al₂O₃ catalyst. This observation revealed that CO, like O₂, interacts with ceria before adsorbing on the Pd surface at 673 K. This is supported by a study on Pt/ceria catalysts which showed that ceria has the ability to uptake CO.^{19,32} Adsorbed CO on Pd can also react with oxygen from ceria.³³

Although the in situ IR technique can be used to probe the dynamics of adsorbed NO and CO as well as the oxidation state of the metal, it cannot be used to directly observe the surface structure or oxidation state of the ceria. We can only infer from literature data that ceria is the key component for uptaking and releasing excess oxygen. Studies using techniques such as XANES/EXAFS³⁴ and XPS^{4,5} have directly observed the changing oxidation state of ceria from Ce₂O₃ to CeO₂ under oxidizing conditions and from CeO₂ to Ce₂O₃ (or oxygen-deficient CeO₂) under reducing conditions.

Reactivity of Adsorbates. The absence of variation in IR intensity of carbonate, nitrate, and chelating nitrate species during CO and O₂ pulses at 473 K (shown in Figure 12) indicates that these species are spectators that are not involved in catalysis of the NO–CO reaction. These species began interacting with CO and O₂ at 673 K (as shown by variation in their intensities in Figures 7 and 9); however, they are not involved in catalytic conversion of NO, as evidenced by lack of relationship between their IR intensity and NO conversion. Pd⁰–NO and linear/bridged CO are the species whose intensities vary with NO conversion during CO and O₂ pulses over Pd/Al₂O₃ and Ce–Pd/Al₂O₃. CO pulses into NO/CO caused replacement of Pd⁰–NO by linear/bridged CO as evidenced by increases in linear/bridged CO with a concomitant decrease in Pd⁰–NO as well as NO conversion; O₂ pulses caused decreases in intensity of linear/bridged CO and Pd⁰–NO as well as NO conversion. The close relationship between Pd⁰–NO intensity and NO conversion suggest that Pd⁰–NO is an active adsorbate involved in NO conversion. This proposition is also supported by a previous selective poisoning/selective enhancement study.²⁶ The replacement of Pd⁰–NO by linear/bridged CO further revealed that both NO and CO compete for the same Pd⁰ sites.^{17,26}

The effect of CO pulsing on NO conversion varied by catalyst and by temperature. Table 3 shows the effect of CO pulsing (Phase I) on both catalysts at 473, 573, and 673 K. Phase I CO pulsing on Ce–Pd/Al₂O₃ caused decreases in NO conversion, indicating that the rate is negative order in CO partial pressure. This is consistent with another recent study on Pd/ceria catalysts.³⁵ However, on Pd/Al₂O₃ at 473 and 573 K, Phase I CO pulses elicited no changes in NO conversion. These different

behaviors suggest that the kinetics for the NO–CO reaction is rather complex and that the elementary steps involved in the reaction are very sensitive to reaction temperature.

Conclusions

Linear NO and linear/bridged CO on Pd⁰ sites are active adsorbates for the NO–CO reaction. Ceria minimizes the effect of the oxidizing (O₂) and reducing agent (CO) on the adsorbates on Ce–Pd/Al₂O₃ at 673 K. This ceria effect diminished at 573 and 473 K. Comparison of oxygen storage during NO–CO reaction from this study and in O₂/CO pulses in helium from literature results show that the presence of adsorbed NO/CO and their decomposition products on the Pd surface lead O₂ and CO to adsorb and react on the ceria surface prior to the Pd⁰ surface. The O₂ pulses at 473 K, unlike those at 673 K, decreased linear/bridged CO and Al–NCO without producing Pd⁺–NO, indicating that oxygen blocks the Pd sites for CO adsorption and for Al–NCO formation without oxidizing Pd⁰ to Pd⁺.

Acknowledgment. This work was supported by the National Science Foundation under Grant CTS-942111996. We thank Mr. Toshitaka Tanabe at Toyota Central R&D Lab for helpful suggestions.

References and Notes

- (1) Shelef, M. *Catal. Rev.—Sci. Eng.* **1994**, *36*, 443.
- (2) Taylor, K. C. *Catal. Rev.—Sci. Eng.* **1993**, *35*, 457.
- (3) Holmgren, A.; Anderson, B. *J. Catal.* **1998**, *178*, 14.
- (4) Schmiege, S. J.; Belton, D. N. *Appl. Catal. B* **1995**, *6*, 127.
- (5) Putna, E. S.; Gorte, R. J.; Vohs, J. M.; Graham, G. W. *J. Catal.* **1998**, *178*, 598.
- (6) Trovarelli, A. *Catal. Rev.—Sci. Eng.* **1996**, *38*, 439.
- (7) Kakuta, N.; Morishima, N.; Kotobuki, M.; Iwase, T.; Mizushima, T.; Sato, Y.; Matsuura, S. *Appl. Surf. Sci.* **1997**, *121/122*, 408.
- (8) Hickey, N.; Fornasiero, P.; Graziani, M.; Blanco, G.; Bernal, S. *Chem. Commun.* **2000**, *5*, 357.
- (9) Monte, R. D.; Fornasiero, P.; Graziani, M.; Kašpar, J. *J. Alloys Compd.* **1998**, *275–277*, 877.
- (10) Yao, H. C.; Yao, Y. F. *J. Catal.* **1984**, *86*, 254.
- (11) Hori, C. E.; Permana, H.; Ng, K. Y. S.; Brenner, A.; More, K.; Rahmoeller, K. M.; Belton, D. *Appl. Catal. B* **1998**, *16*, 105.
- (12) Cho, B. K. *J. Catal.* **1991**, *131*, 74.
- (13) Chuang, S. S. C.; Brundage, M. A.; Balakos, M. W.; Srinivas, G. *Appl. Spectrosc.* **1995**, *49*, 1151.
- (14) Oh, S. H. *J. Catal.* **1990**, *124*, 477.
- (15) Grill, C. M.; Gonzalez, R. D. *J. Phys. Chem.* **1980**, *84*, 878.
- (16) Palazov, A.; Chang, C. C.; Kokes, R. J. *J. Catal.* **1975**, *36*, 338.
- (17) Almusateer, K.; Chuang, S. S. C. *J. Catal.* **1999**, *184*, 189.
- (18) Kikuzono, B. Y.; Kagami, S.; Naito, S.; Onishi, T.; Tamaru, K. *Faraday Discuss. Chem. Soc.* **1982**, *72*, 135.
- (19) Binet, C.; Badri, A.; Boutonnet-Kizling, M.; Lavalley, J. C. *J. Chem. Soc., Faraday Trans.* **1994**, *90*, 1023.
- (20) Raval, R.; Blyholder, G.; Haq, S.; King, D. A. *J. Phys. Condens. Matter* **1989**, *1*, SB165.
- (21) Unland, M. L. *J. Catal.* **1973**, *31*, 459.
- (22) Solymosi, F.; Rasko, J. *J. Catal.* **1980**, *63*, 217.
- (23) Hecker, W. C.; Bell, A. T. *J. Catal.* **1984**, *85*, 389.
- (24) Nakamoto, K. *Infrared and Raman Spectra of Inorganic and Coordination Compounds*; Wiley: New York, 1986.
- (25) Bensalem, A.; Muller, J.-C.; Tessier, D.; Bozon-Verduraz, F. *J. Chem. Soc., Faraday Trans.* **1996**, *92*, 3233.
- (26) Almusateer, K.; Chuang, S. S. C. *J. Catal.* **1998**, *180*, 161.
- (27) Krishnamurthy, R.; Chuang, S. S. C.; Balakos, M. W. *J. Catal.* **1995**, *157*, 512.
- (28) Chuang, S. S. C.; Tan, C.-D. *J. Catal.* **1998**, *173*, 95.
- (29) Nibbelke, R. H.; Nievergeld, A. J. L.; Hoebink, J. H. B. J.; Martin, G. B. *Appl. Catal. B* **1998**, *19*, 245.
- (30) Rodriguez, J. A.; Goodman, D. W. *Surf. Sci. Rep.* **1991**, *14*, 27.
- (31) McCabe, R. W.; Jen, H.-W.; Chun, W.; Graham, G. W.; Haack, L. P.; Straccia, A.; Benson, D. *Appl. Catal. A* **1999**, *184*, 265.
- (32) Holmgren, A.; Andersson, B.; Duprez, D. *Appl. Catal. B* **1999**, *22*, 215.
- (33) Cordatos, H.; Gorte, J. *J. Catal.* **1996**, *159*, 112.
- (34) Holles, J. H.; Davis, R. J. *J. Phys. Chem. B* **2000**, *104*, 9653.
- (35) Holles, J. H.; Davis, R. J.; Murray, T. M.; Howe, J. M. *J. Catal.* **2000**, *195*, 193.